havior for $k$ near 2; for large $k$ (8) and (10) show that $\sigma$ increases like log $k$.

These results have to be compared with the results of Jäger and Hulme which are also indicated in the figures. They have given curves for the dipole up to $k=7$ and for the quadripole up to $k=5$ in the case $Z=84$. One sees again that by the combined use of the Born and Schrödinger approximation results the total internal conversion coefficient may be obtained for all $k$ and all $Z$ to within a fair degree of accuracy, say of the order 15 percent.

---

AUGUST 1, 1935 PHYSICAL REVIEW VOLUME 48

# The Spectrum of Molybdenum V

M. W. Trawick, *Department of Physics, Cornell University*

(Received June 15, 1935)

The spectrum of Mo V has been excited in a vacuum spark and photographed with a vacuum spectrograph. With the aid of the irregular doublet law applied to the Sr I-like isoelectronic sequence, lines involving combinations of $4d^2\,{}^3(FP)$, $4d5s\,{}^{1,3}D$, $4d5d\,{}^1(PD)$, and $4d5d\,{}^3(DF)$ with $4d5p\,{}^{3,1}(F^\circ D^\circ P^\circ)$ and $4d4f\,{}^3(G^\circ F^\circ)$, and lying in the spectral region from 2100A to 400A have been identified. Estimates of the absolute term values have been made from a Moseley diagram.

THE spectra of the first four elements in the Sr I-like isoelectronic sequence have been classified by various investigators; Sr I by Russell and Saunders and by others,[1] Y II by Meggers and Russell,[2] Zr III by Kiess and Lang,[3] and Cb IV by Gibbs and White[4] and, more fully, by Lang.[5] The present paper extends the sequence to include Mo V.

The spectrum of Mo V was excited in a vacuum spark between solid metal electrodes and photographed with a vacuum spectrograph containing a concave grating of 150-cm radius of curvature and ruled with 15,000 lines per inch. The vacuum spark between aluminum electrodes furnished the standard lines, either those of aluminum itself or those of nitrogen and oxygen brought out in the discharge.

Higher order lines were carefully noted. The lines of Mo IV and Mo VI which lie in the region investigated (2100A to 400A) were sorted out on the basis of the classifications by Eliason[6] and by the author.[7]

The identification of the multiplet transitions $4d5p\,{}^3(F^\circ D^\circ P^\circ)$ into $4d^2\,{}^3(FP)$ and $4d5s\,{}^3D$ furnished the key to the classification of the triplet lines. First, the triplet transition $4d5s\,{}^3D - 4d5p\,{}^3(F^\circ D^\circ P^\circ)$ was looked for with the help of a linear extrapolation of the wave numbers of the corresponding lines for the preceding members of the sequence. Fig. 1 is a diagram showing the relative positions of the lines in these multiplets. In this diagram, only the stronger lines, in general, are connected from one element to the next.

Since there was a large number of lines in the region of the spectrum occupied by the lines of the $4d5s\,{}^3D - 4d5p\,{}^3(F^\circ D^\circ P^\circ)$ multiplets, it was only by finding lines lying in the region of $4d^2\,{}^3F - 4d5p\,{}^3(F^\circ D^\circ P^\circ)$ (as indicated by the linear extrapolation of wave numbers) and having the same wave number separations as the lines of the $4d5s - 4d5p$ transition that a solution of the problem was obtained. Difficulty in identifying these latter lines was experienced because

[1] Saunders, Astrophys. J. **56**, 73 (1922); Russell and Saunders, Astrophys. J. **61**, 39 (1925).
[2] Meggers and Russell, Bur. Standards J. Research **2**, 733 (1929).
[3] Kiess and Lang, Bur. Standards J. Research **5**, 305 (1930)
[4] Gibbs and White, Phys. Rev. **31**, 520 (1928).
[5] Lang, Phys. Rev. **44**, 325 (1933). Also, private communication to Professor R. C. Gibbs.
[6] Eliason, Phys. Rev. **43**, 745 (1933).
[7] Trawick, Phys. Rev. **46**, 63 (1934).

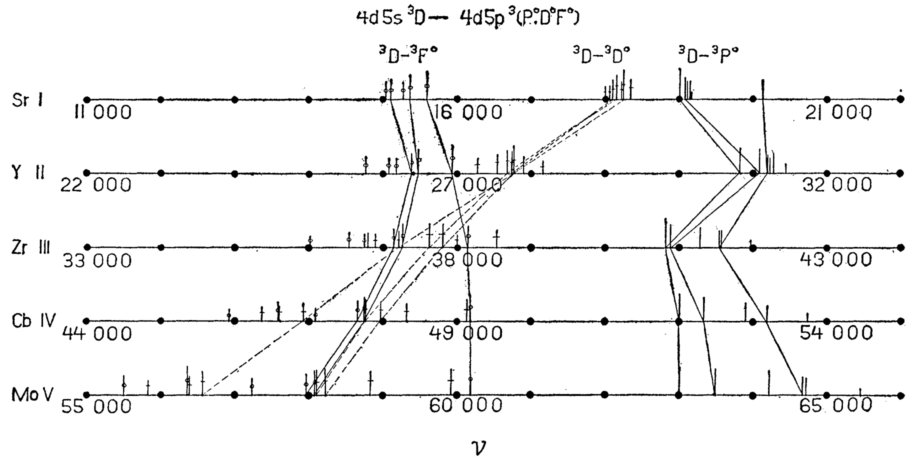


FIG. 1. Displacement of multiplets.

TABLE I. *Classified lines of Mo V.*

| λ(A) | Int. | ν(cm⁻¹) | Classification | λ(A) | Int. | ν(cm⁻¹) | Classification |
|---|---|---|---|---|---|---|---|
| 2159.30 | 0*d* | 46,311.3 | $4d5s\ ^3D_3 - 4d5p\ ^1F^\circ_3$ | 1189.96 | 2 | 84,036.4 | $4d5p\ ^3F^\circ_4 - 4d5d\ ^3F_3$ |
| 2081.83 | 5*d* | 48,034.6 | $4d5s\ ^3D_2 - 4d5p\ ^1F^\circ_3$ | 1169.34 | 4 | 85,518.3 | $4d5p\ ^3F^\circ_3 - 4d5d\ ^3F_2$ |
| 1848.59 | 0 | 54,095.3 | $4d5s\ ^3D_2 - 4d5p\ ^1P^\circ_1$ | 1157.85 | 4*d* | 86,367.0 | $4d5p\ ^3F^\circ_2 - 4d5d\ ^3F_2$ |
| 1823.98 | 0 | 54,825.2 | $4d5s\ ^3D_1 - 4d5p\ ^1P^\circ_1$ | 1148.53 | 8*d* | 87,067.8 | $4d5p\ ^3F^\circ_4 - 4d5d\ ^3F_4$ |
| 1801.49 | 5 | 55,509.6 | $4d5s\ ^3D_3 - 4d5p\ ^3F^\circ_2$ | 1137.97 | 6*d* | 87,875.8 | $4d5p\ ^3F^\circ_3 - 4d5d\ ^3F_3$ |
| 1790.91 | 4 | 55,837.5 | $4d5s\ ^3D_2 - 4d5p\ ^3D^\circ_1$ | 1127.07 | 0 | 88,725.0 | $4d5p\ ^3F^\circ_2 - 4d5d\ ^3F_3$ |
| 1774.35 | 9 | 56,358.7 | $4d5s\ ^3D_3 - 4d5p\ ^3F^\circ_3$ | 1099.97 | 0 | 90,911.6 | $4d5p\ ^3F^\circ_3 - 4d5d\ ^3F_4$ |
| 1773.79 | 4*d* | 56,376.4 | $4d5s\ ^3D_3 - 4d5p\ ^3D^\circ_2$ | 730.27 | 1 | 136,936 | $4d^2\ ^3P_2 - 4d5p\ ^3F^\circ_2$ |
| 1767.77 | 7 | 56,568.4 | $4d5s\ ^3D_1 - 4d5p\ ^3D^\circ_1$ | 729.23 | 1 | 137,131 | $4d^2\ ^3P_1 - 4d5p\ ^3D^\circ_1$ |
| 1756.83 | 2*d* | 56,920.7 | $4d5s\ ^3D_3 - 4d5p\ ^1D^\circ_2$ | 725.77 | 8 | 137,785 | $4d^2\ ^3P_0 - 4d5p\ ^3D^\circ_1$<br>$4d^2\ ^3P_2 - 4d5p\ ^3F^\circ_3$ |
| 1756.33 | 1 | 56,936.9 | $4d5p\ ^3P^\circ_2 - 4d5d\ ^3D_1$ | 721.86 | 8 | 138,534 | $4d^2\ ^3P_1 - 4d5p\ ^3F^\circ_2$ |
| 1749.02 | 2 | 57,174.9 | $4d5s\ ^1D_2 - 4d5p\ ^1F^\circ_3$ | 717.36 | 3 | 139,400 | $4d^2\ ^3P_1 - 4d5p\ ^3D^\circ_2$ |
| 1747.22 | 7 | 57,233.8 | $4d5s\ ^3D_2 - 4d5p\ ^3F^\circ_2$ | 716.19 | 7 | 139,628 | $4d^2\ ^3P_2 - 4d5p\ ^3D^\circ_3$ |
| *1725.15 | 6 | 57,966.0 | $4d5s\ ^3D_1 - 4d5p\ ^3F^\circ_2$ | 698.33 | 2 | 143,199 | $4d^2\ ^3P_2 - 4d5p\ ^3P^\circ_1$ |
| 1722.40 | 2 | 58,058.5 | $4d5p\ ^3P^\circ_1 - 4d5d\ ^3D_2$ | 692.32 | 6 | 144,442 | $4d^2\ ^3P_2 - 4d5p\ ^3P^\circ_2$ |
| 1721.67 | 7 | 58,083.1 | $4d5s\ ^3D_2 - 4d5p\ ^3F^\circ_3$ | 690.59 | 6 | 144,804 | $4d^2\ ^3P_1 - 4d5p\ ^3P^\circ_1$ |
| 1721.20 | 7 | 58,099.0 | $4d5s\ ^3D_2 - 4d5p\ ^3D^\circ_2$ | 688.47 | 6 | 145,250 | $4d^2\ ^3P_1 - 4d5p\ ^3P^\circ_0$ |
| 1718.09 | 7 | 58,204.2 | $4d5s\ ^3D_3 - 4d5p\ ^3D^\circ_3$ | 687.52 | 3 | 145,450 | $4d^2\ ^3P_0 - 4d5p\ ^3P^\circ_1$ |
| 1705.25 | 0 | 58,642.4 | $4d5s\ ^3D_2 - 4d5p\ ^1D^\circ_2$ | 684.75 | 5 | 146,039 | $4d^2\ ^3P_1 - 4d5p\ ^3P^\circ_2$ |
| 1699.75 | 7 | 58,832.2 | $4d5s\ ^3D_1 - 4d5p\ ^3D^\circ_2$ | 676.42 | 6 | 147,837 | $4d^2\ ^3F_4 - 4d5p\ ^3F^\circ_3$ |
| 1684.16 | 00 | 59,376.8 | $4d5s\ ^3D_1 - 4d5p\ ^1D^\circ_2$ | 672.24 | 6 | 148,756 | $4d^2\ ^3F_3 - 4d5p\ ^3F^\circ_2$ |
| 1668.67 | 6 | 59,928.0 | $4d5s\ ^3D_2 - 4d5p\ ^3D^\circ_3$ | 671.37 | 6 | 148,949 | $4d^2\ ^3F_2 - 4d5p\ ^3D^\circ_1$ |
| 1661.23 | 9 | 60,196.4 | $4d5s\ ^3D_3 - 4d5p\ ^3F^\circ_4$ | *668.39 | 10 | 149,613 | $4d^2\ ^3F_3 - 4d5p\ ^3F^\circ_3$ |
| 1644.74 | 6 | 60,799.9 | $4d5p\ ^3D^\circ_3 - 4d5d\ ^3D_3$ | *668.32 | 10 | 149,629 | $4d^2\ ^3F_3 - 4d5p\ ^3D^\circ_2$ |
| 1643.12 | 2 | 60,859.8 | $4d5p\ ^1D^\circ_2 - 4d5d\ ^1D_2$ | 668.09 | 10 | 149,680 | $4d^2\ ^3F_4 - 4d5p\ ^3D^\circ_3$ |
| 1622.55 | 0 | 61,631.4 | $4d5p\ ^3D^\circ_3 - 4d5d\ ^3D_2$ | 665.14 | 6 | 150,344 | $4d^2\ ^3F_2 - 4d5p\ ^3F^\circ_2$ |
| 1596.73 | 0 | 62,628.0 | $4d5p\ ^3D^\circ_2 - 4d5d\ ^3D_3$ | *661.40 | 4 | 151,193 | $4d^2\ ^3F_2 - 4d5p\ ^3F^\circ_3$ |
| 1586.91 | 8 | 63,015.5 | $4d5s\ ^3D_3 - 4d5p\ ^3P^\circ_2$ | *661.33 | 4 | 151,209 | $4d^2\ ^3F_2 - 4d5p\ ^3D^\circ_2$ |
| 1581.34 | 6 | 63,237.5 | $4d5s\ ^1D_2 - 4d5p\ ^1P^\circ_1$ | 660.28 | 1 | 151,451 | $4d^2\ ^3F_3 - 4d5p\ ^3D^\circ_3$ |
| 1575.85 | 2 | 63,457.8 | $4d5p\ ^3D^\circ_2 - 4d5d\ ^3D_2$ | 659.31 | 7 | 151,674 | $4d^2\ ^3F_4 - 4d5p\ ^3F^\circ_4$ |
| 1574.71 | 8 | 63,503.8 | $4d5s\ ^3D_2 - 4d5p\ ^3P^\circ_1$ | 651.68 | 2 | 153,450 | $4d^2\ ^3F_3 - 4d5p\ ^3F^\circ_4$ |
| 1572.96 | 3 | 63,574.4 | $4d5p\ ^3D^\circ_2 - 4d5d\ ^3D_1$ | 639.95 | 2 | 156,262 | $4d^2\ ^3F_3 - 4d5p\ ^3P^\circ_2$ |
| 1559.70 | 3 | 64,114.9 | $4d5p\ ^1D^\circ_2 - 4d5d\ ^1P_1$ | 638.51 | 0 | 156,615 | $4d^2\ ^3F_2 - 4d5p\ ^3P^\circ_1$ |
| 1556.78 | 6 | 64,235.2 | $4d5s\ ^3D_1 - 4d5p\ ^3P^\circ_1$ | 434.52 | 6 | 230,139 | $4d^2\ ^3F_3 - 4d4f\ ^3F^\circ_2$ |
| 1546.13 | 4 | 64,677.6 | $4d5s\ ^3D_1 - 4d5p\ ^3P^\circ_0$ | 431.55 | 6 | 231,723 | $4d^2\ ^3F_2 - 4d4f\ ^3F^\circ_2$ |
| 1544.65 | 4 | 64,739.6 | $4d5s\ ^3D_2 - 4d5p\ ^3P^\circ_2$ | 428.63 | 3 | 233,301 | $4d^2\ ^3F_3 - 4d4f\ ^3F^\circ_3$ |
| 1538.75 | 0 | 64,987.8 | $4d5s\ ^1D_2 - 4d5p\ ^3D^\circ_1$ | 425.77 | 0 | 234,869 | $4d^2\ ^3F_2 - 4d4f\ ^3F^\circ_3$ |
| 1528.80 | 3 | 65,410.8 | $4d5p\ ^1P^\circ_1 - 4d5d\ ^1D_2$ | 420.61 | 5 | 237,750 | $4d^2\ ^3F_4 - 4d4f\ ^3F^\circ_4$ |
| 1527.44 | 0 | 65,469.0 | $4d5s\ ^3D_1 - 4d5p\ ^3P^\circ_2$ | 417.49 | 6 | 239,527 | $4d^2\ ^3F_3 - 4d4f\ ^3F^\circ_4$ |
| 1521.51 | 1 | 65,724.2 | $4d5p\ ^3D^\circ_1 - 4d5d\ ^3D_2$ | 414.11 | 0 | 241,482 | $4d^2\ ^3F_4 - 4d4f\ ^3G^\circ_4$ |
| 1518.86 | 3 | 65,838.9 | $4d5p\ ^3D^\circ_1 - 4d5d\ ^3D_1$ | 413.11 | 0 | 242,055 | $4d^2\ ^3F_3 - 4d4f\ ^3G^\circ_3$ |
| 1487.18 | 0 | 67,241.4 | $4d5s\ ^1D_2 - 4d5p\ ^3D^\circ_2$ | 412.42 | 5 | 242,471 | $4d^2\ ^3F_4 - 4d4f\ ^3G^\circ_5$ |
| 1475.19 | 2 | 67,787.9 | $4d5s\ ^1D_2 - 4d5p\ ^1D^\circ_2$ | *411.08 | 8 | 243,255 | $4d^2\ ^3F_3 - 4d4f\ ^3G^\circ_4$ |
| 1456.35 | 3 | 68,664.8 | $4d5p\ ^1P^\circ_1 - 4d5d\ ^1P_1$ | 410.35 | 5 | 243,665 | $4d^2\ ^3F_2 - 4d4f\ ^3G^\circ_3$ |
| 1447.78 | 00 | 69,071.3 | $4d5s\ ^1D_2 - 4d5p\ ^3D^\circ_3$ | | | | |
| 1399.14 | 3 | 71,472.5 | $4d5p\ ^1F^\circ_3 - 4d5d\ ^1D_2$ | | | | |

several of the principal lines belonging to these groups were not resolved on the plates.

The identification of the remainder of the lines was facilitated by determining the narrow region in which they must lie by use of diagrams similar to Fig. 1 for the corresponding transitions in the other members of the sequence.

The singlets were identified by finding the transitions of $4d5p\ ^1(P^\circ D^\circ F^\circ)$ into $4d5s\ ^3D$. After these lines had been identified, it was possible

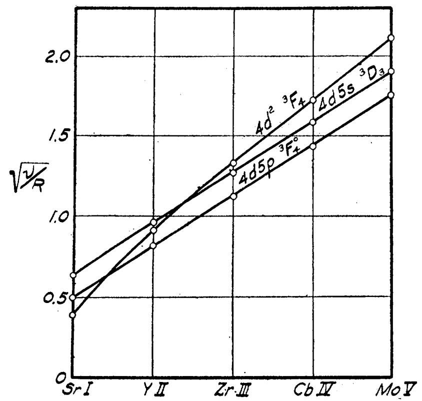


FIG. 2. Moseley diagram.

to determine the $4d5s\ ^1D$ and $4d5d\ ^1(PD)$ terms by their combinations with the $4d5p$ singlets. The $4d^2\ ^1(FP)$ terms were not found, as the lines yielded by the combinations they make with the $4d5p$ singlets lie at shorter wavelengths than it was possible to photograph successfully.

Table I gives a list of the classified lines, with their relative intensities and wave numbers. The lines not completely resolved from other lines very near them are marked with asterisks.

Approximate absolute term values were assigned from extrapolations on a Moseley diagram, Fig. 2. The values found by extrapolation

TABLE II. *Term values for Mo V.*

| CONFIG. | TERM | RELATIVE TERM VALUES | APPROXIMATE ABSOLUTE TERM VALUES | CONFIG. | TERM | RELATIVE TERM VALUES | APPROXIMATE ABSOLUTE TERM VALUES |
|---|---|---|---|---|---|---|---|
| $4d^2$ | $^3F_2$ | 0 | 493,359 | $4d5p$ | $^3F^\circ_4$ | 155,033 | 338,326 |
| | $^3F_3$ | 1,585 | 491,774 | | $^3P^\circ_1$ | 156,616 | 336,743 |
| | $^3F_4$ | 3,359 | 490,000 | | $^3P^\circ_0$ | 157,060 | 336,299 |
| | $^3P_0$ | 11,165 | 482,194 | | $^3P^\circ_2$ | 157,852 | 335,507 |
| | $^3P_1$ | 11,812 | 481,547 | | | | |
| | $^3P_2$ | 13,413 | 479,946 | $4d5d$ | $^1D_2$ | 212,620 | 280,739 |
| | | | | | $^3D_3$ | 213,840 | 279,517 |
| $4d5s$ | $^1D_2$ | 83,971 | 409,388 | | $^3D_2$ | 214,671 | 278,688 |
| | $^3D_1$ | 92,381 | 400,978 | | $^3D_1$ | 214,786 | 278,571 |
| | $^3D_2$ | 93,113 | 400,246 | | $^1P_1$ | 215,874 | 277,485 |
| | $^3D_3$ | 94,837 | 398,522 | | $^3F_2$ | 236.714 | 256,645 |
| | | | | | $^3F_3$ | 239,071 | 254,288 |
| $4d5p$ | $^1F^\circ_3$ | 141,150 | 352,209 | | $^3F_4$ | 242,104 | 251,255 |
| | $^1P^\circ_1$ | 147,209 | 346,150 | | | | |
| | $^3D^\circ_1$ | 148,950 | 344,409 | $4d4f$ | $^3F^\circ_2$ | 231,724 | 261,635 |
| | $^3F^\circ_2$ | 150,346 | 343,013 | | $^3F^\circ_3$ | 234,886 | 258,473 |
| | $^3F^\circ_3$ | 151,196 | 342,163 | | $^3F^\circ_4$ | 241,112 | 252,247 |
| | $^3D^\circ_2$ | 151,212 | 342,147 | | $^3G^\circ_3$ | 243,665 | 249,694 |
| | $^1D^\circ_2$ | 151,760 | 341,599 | | $^3G^\circ_4$ | 244,[illegible]41 | 248,518 |
| | $^3D^\circ_3$ | 153,041 | 340,318 | | $^3G^\circ_5$ | 245,830 | 247,529 |

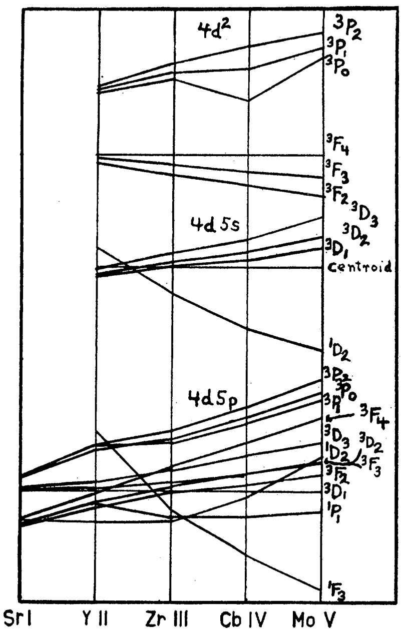


FIG. 3. Relative positions of terms in the configurations.

of $(4d^2\ ^3F_4/R)^{\frac{1}{2}}$, $(4d5s\ ^3D_3/R)^{\frac{1}{2}}$, and $(4d5p\ ^3F^\circ_4/R)^{\frac{1}{2}}$ gave the most consistent results and are the only ones shown in Fig. 2. The absolute term values estimated by this method and referred to $4d\ ^2D_{1\frac{1}{2}}$ of Mo VI along with the term values relative to $4d^2\ ^3F_2$, the lowest term actually found, are given in Table II.

Fig. 3 shows the terms of each configuration throughout the sequence plotted relative to one of the terms of that configuration or to the centroid of the configuration in the case in which all the terms of that configuration were found. The terms for Mo V seem to be related to each other and to the terms of the preceding elements in a manner to be expected, except for an apparent irregularity in the Cb IV $4d^2\ ^3P_{0,\ 1}$.

The writer wishes to thank Professor R. C. Gibbs for suggesting the problem and for giving much helpful advice in connection with the work. He is deeply indebted to Professor R. J. Lang for his kindness in supplying Professor Gibbs with his unpublished data on Cb IV which have been utilized in the composition of Figs. 1, 2 and 3.